Vol 15 No 7, July 2006
1009-1963/2006/15(07)/1585-06

Chinese Physics

© 2006 Chin. Phys. Soc.
and IOP Publishing Ltd

# First principles study on the structural, electronic and optical properties of diluted magnetic semiconductors $Zn_{1-x}Co_xX$ ($X$=S, Se, Te)*

Ouyang Chu-Ying(欧阳楚英)[a)b)], Xiong Zhi-Hua(熊志华)[a)b)†],
Ouyang Qi-Zhen(欧阳企振)[a)], Liu Guo-Dong(刘国栋)[b)],
Ye Zhi-Qing(叶志清)[a)], and Lei Min-Sheng(雷敏生)[a)]

[a)] *Department of Physics, Jiangxi Normal University, Nanchang* 330027, *China*
[b)] *Key Laboratory for Opto-electronics of Jiangxi Province, Jiangxi Science & Technology Normal University, Nanchang* 330013, *China*

(Received 22 December 2005; revised manuscript received 3 April 2006)

The electronic and optical properties of zincblende Zn$X$($X$=S, Se, Te) and Zn$X$:Co are studied from density functional theory (DFT) based first principles calculations. The local crystal structure changes around the Co atoms in the lattice are studied after Co atoms are doped. It is shown that the Co-doped materials have smaller lattice constant (about 0.6%–0.9%). This is mainly due to the shortened Co–$X$ bond length. The (partial) density of states (DOS) is calculated and differences between the pure and doped materials are studied. Results show that for the Co-doped materials, the valence bands are moving upward due to the existence of Co 3d electron states while the conductance bands are moving downward due to the reduced lattice constants. This results in the narrowed band gap of the doped materials. The complex dielectric indices and the absorption coefficients are calculated to examine the influences of the Co atoms on the optical properties. Results show that for the Co-doped materials, the absorption peaks in the high wavelength region are not as sharp and distinct as the undoped materials, and the absorption ranges are extended to even higher wavelength region.

**Keywords:** first principles, diluted magnetic semiconductors, optical properties, electronic properties
**PACC:** 7115A, 7550P, 7000, 3620K

## 1. Introduction

Diluted magnetic semiconductors (DMS) constitute a class of semiconducting materials formed by randomly replacing some of the cations in II–VI or III–V compounds with magnetic transition metal ions (e.g. Fe, Co, or Mn). From the very beginning, they attracted the attention of many investigators, because of their remarkable magnetic and optical properties,[1−8] and now they are very interesting materials for applications in spin electronics.[9−12] In the past 20 years, DMS materials have been extensively studied, both experimentally [13−15] and theoretically.[16−18]

As transition metal ions are implanted into the compound semiconductors and replace other cations in the lattice, the most direct influence is on the local structural distortion of the crystal, and the Jahn–Teller effect will be an important factor to the optical transitions. As early as 1978, Uba and Baranowski[19] reported the dynamic and static Jahn–Teller effect that influences the $^4T_1$ multiplet of $Co^{2+}$ in ZnSe. Iwanowski *et al* [20] studied the radii of the transition metal ions in ZnS: $M$($M$=Mn, Fe, Co, Ni) crystal by extended x-ray absorption fine structures, but they did not provide detailed ionic positions and the position changes of the surrounding atoms. Dreyhsig and Litzenburger[2] proposed the charge-transfer concept to explain the optical transitions of ZnS:$Co^{2+}$. However, their theoretical framework is not from a first principles basis, and they also did not reveal the local environment of $Co^{2+}$ cations in the compound.

Although several empirical and semiempirical theoretical studies on the basic properties of DMS have been reported, there are, however, still some unclear points concerning these materials. To our knowl-

*Project supported by the National Natural Science Foundation of China (Grant No 10564002) and the Open Foundations of Key Laboratory for Opto–electronics of Jiangxi Province, China (Grant Nos 2004003 and 2004008), the Natural Science Foundation of Jiangxi Province, China (Grant No 0512017) and the Youth Science Program of Jiangxi Normal University, China(Grant No 1075).

†E-mail: xiong_zhihua@126.com

edge, no investigator has ever systematically studied the local distortion of the crystal after the transition metal ions are implanted into the compound, and to what extent the lattice distortion will influence its electronic and optical properties. In the present paper, we shall systematically study the structural properties of DMS $Zn_{1-x}Co_xX$ ($X$=S, Se, Te) from first principles calculations, and the influence of the structural distortion on the electronic and optical properties after $Co^{2+}$ are implanted into the crystal.

## 2. Computational details

The density functional theory based first principles calculations are performed using the Vienna *ab initio* simulation package VASP.[21,22] This code solves the Kohn–Sham equations within the pseudopotential approximation[23] and the generalized gradient approximation (GGA). The ultra-soft pseudopotentials[24] are employed in this paper. The valence electrons are expanded in a plane wave basis set and the effect of the core states on the valence electrons is treated with ultrasoft pseudopotentials. The pseudopotentials for II–VI semiconductors have been carefully treated in the present study. As the core–valence charge overlap is significant, the outlying cation d states cannot be considered as true core states. In this case, we need to use finer grid in real space and more than doubling the required number of valence electrons, although it greatly increases the computational load.[25] The Perdew–Wang exchange–correlation functional (PW91)[26] is used for the calculation of the electron exchange correlation energy.

All the calculations are performed in a 2 × 2 × 2 supercell, which includes 64 atoms. For the case of Zn$X$:$Co^{2+}$, one Zn atom in the centre of the lattice, with fractional coordinates (0.5, 0.5, 0.5), is replaced by one Co atom. The convergence tests of the total energy with respect to the plane wave energy cutoff and $k$-points sampling have been carefully examined. The final set of energies are computed with an energy cutoff of 520 eV, and the integration is performed using 3 × 3 × 3 $k$-points sampling over the irreducible Brillouin zone, generated by the Monkhorst–Pack scheme.[27] The computed energy is found to converge better than 0.002 eV/atom with these parameters. The electronic ground state is determined through conjugate gradient minimization of the total energy with respect to the plane wave coefficients. Since the matrix element usually changes more rapidly within the Brillouin zone than electronic energies themselves, it is important to use sufficient number of $k$-points in the Brillouin zone when running optical matrix element calculations. Therefore, in the calculations of the optical properties, the Monkhorst–Pack grid is chosen to be 5 × 5 × 5. After the $Co^{2+}$ ion is implanted into the crystal and replaces one $Zn^{2+}$, the ionic positions, lattice parameters and cell volume are fully relaxed, and the final forces on all relaxed atoms are less than 0.02 eV/Å.

## 3. Results and discussion

### 3.1. The local structural distortion around $Co^{2+}$ in the crystal

The cubic structure of the zincblende Zn$X$ structure with space group $T_d^2$ can be described with $a = b = c$ and $\alpha = \beta = \gamma = 90°$. In the 2 × 2 × 2 supercell, after one $Zn^{2+}$ was replaced by one $Co^{2+}$, the shape of the cubic structure is kept unchanged ($\alpha = \beta = \gamma = 90°$), only the lattice constant and the local atomic positions are changed.

Shown in Table 1 are the optimized crystal parameters of Zn$X$ and Zn$X$:$Co^{2+}$, which will be used for further calculation.

**Table 1.** The relaxed crystal structures of Zn$X$ and Zn$X$: $Co^{2+}$

| lattice constant/Å | ZnS | ZnCoS | ZnSe | ZnCoSe | ZnTe | ZnCoTe |
|---|---|---|---|---|---|---|
| Calculated (2a) | 5.361 | 5.327 | 5.623 | 5.590 | 6.079 | 6.025 |
| Exp. [28−30] | 5.414 | - | 5.668 | - | 6.102 | - |
| Other work [31] | 5.345 | - | 5.618 | - | 6.045 | - |
| Zn-$X$ | 2.326 | - | 2.440 | - | 2.634 | - |
| Co-$X$ | - | 2.205 | - | 2.304 | - | 2.465 |

Compared with the experimental value, the calculated values are a little lower (0.8%–1%), which are within the scope of the allowed errors. And the lattice constant of Zn$X$ are in good agreement with other calculated results. The lattice constant of the Co-doped materials is a little smaller (0.6%–0.9%) than that of the undoped ones. From checking the relative atomic positions we can easily find out that the reduced lattice constant is mainly due to the smaller bond length of the Co–$X$ bonds, which in turn breaks the crystal symmetry in local area, as shown in Fig.1.

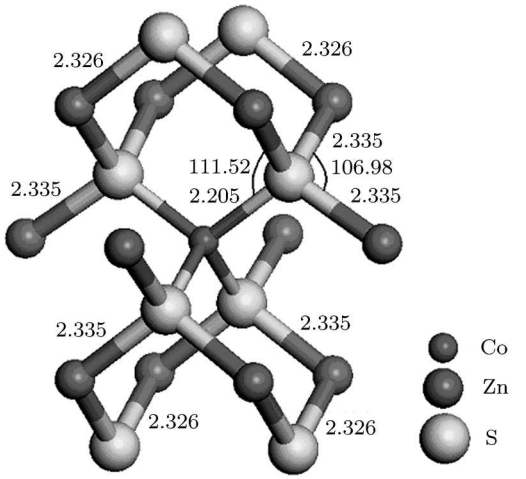



**Fig.1.** The distorted local structure of ZnS:$Co^{2+}$ around the central Co atom that replaces a Zn atom in the lattice.

As can be seen from Fig.1 and Table 1, the Co–S bond length is 2.205 Å, which is much smaller than that of the average Zn–S bond length. This indicates the stronger Co–S interactions in the lattice. The tetrahedral structures around the S atoms that are connected with the centred Co atom are distorted. The Zn–S bond length for the S atoms that are connected with the Co atom is 2.335 Å, which is larger than the average S–Zn bond length. However, the S–Zn bond length decreases to 2.326 Å when it extends far away from the central Co atom. Furthermore, the distorted tetrahedral structure can also be characterized by the angles, as indicated in Fig.1, which is deviated from the standard tetrahedron's 109.47 degrees.

## 3.2. Electronic properties

The electronic structures of Zn$X$ and Zn$X$:Co ($X$=S, Se, Te) can be described by the total density of states (DOS) and partial density of states (PDOS). Gaussian smearing method is used for the calculation of the DOS, and the broadened width is 0.05 eV. In the following discussion, all the DOS figures are plotted with the Fermi level being taken to be zero.

Figure 2 compares the total DOS of Zn$X$ ($X$=S, Se, and Te) before and after Co atoms are doped. Figure 2(b) shows the DOS around the Fermi level. It can be seen from the figures that the overall shape of the DOS for the doped and undoped Zn$X$ are quite similar, except that the energy levels of the doped Zn$X$ are shifted a little below those of the undoped one.

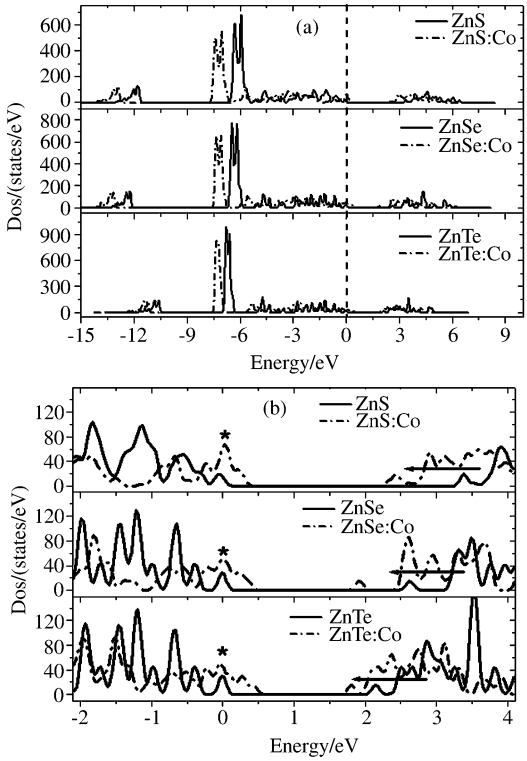



**Fig.2.** The calculated total DOS of Zn$X$ and Zn$X$:Co (a) and DOS around the Fermi level (b). The Fermi level is taken to be zero.

This is mainly due to the reduction of lattice constant of the Zn$X$:Co crystal. Furthermore, the energy levels around the Fermi level are changed a lot after the Co atoms are doped, as can be seen from Fig.2(b). The energy level changes around the Fermi level makes the band gap change a lot, which results in a much lower band gap for the doped materials. The band gaps of Zn$X$ and Zn$X$:Co are listed in Table 2, from which we see that the predicted band gaps are to some extent underestimated as compared with the experimental values.[32−34] This is due to the theoretical framework itself (GGA+USPP), which is generally accepted. Furthermore, the width of the band gap of Co-doped materials is much lower than that of the undoped ones. From Fig.2(b), it can be seen that the reduction of band gaps results from two aspects: 1) for the Co-doped materials, due to the compressed lattice constant, the conduction band moves down and

the valence band moves up, as marked by the arrows in Fig.2(b); 2) the value of the DOS in the valence band near the Fermi level is much larger, as marked by the stars in the figure. This is the result of the Co 3d electron states that can be seen more clearly from the PDOS as shown in Fig.3.

**Table 2.**The band gaps of Zn$X$ and Co-doped Zn$X$

| band gap/eV | ZnS | ZnS: Co | ZnSe | ZnSe:Co | ZnTe | ZnTe: Co |
|---|---|---|---|---|---|---|
| Calculated | 3.24 | 1.85 | 2.43 | 1.30 | 1.95 | 1.18 |
| Exp [32−34] | 3.72 | - | 2.72 | - | 2.39 | - |

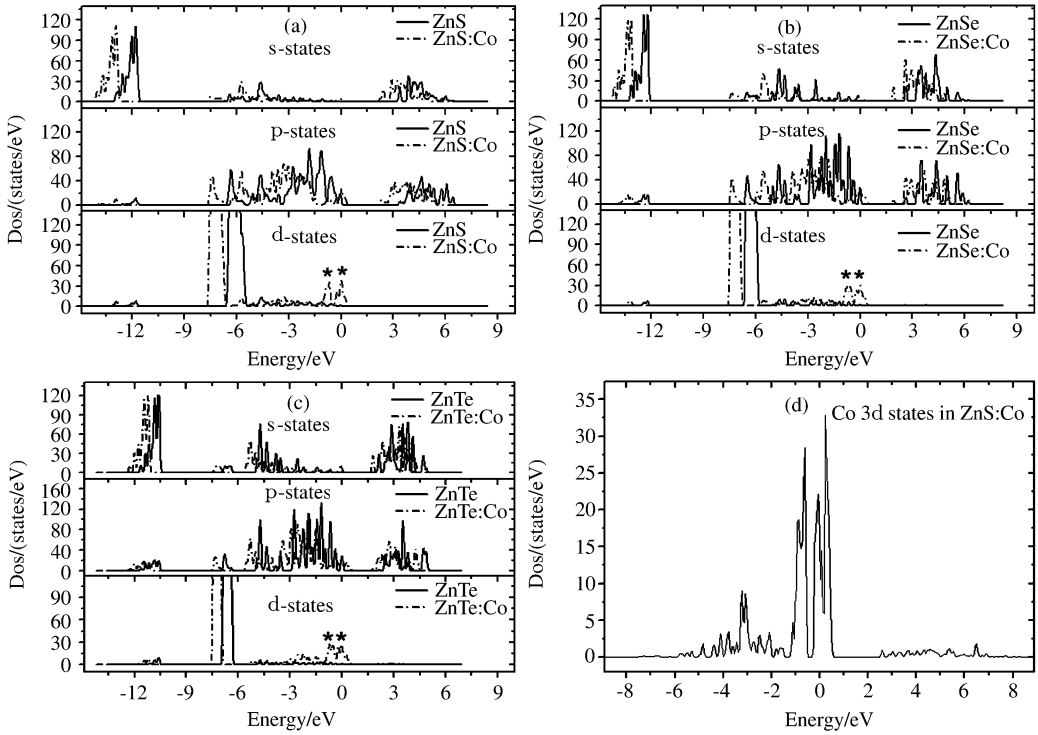



**Fig.3.** Partial DOS of (a) ZnS and ZnS:Co, (b) ZnSe and ZnSe:Co, (c) ZnTe and ZnTe:Co and (d) the Co 3d states in the case of ZnS:Co. In all Co-doped cases, the Co 3d contribution to the valence band around the Fermi level are marked by stars.

Figure 3 is the partial DOS for s, p and d states of Zn$X$ and ZnX:Co. In Fig.3 the differences between Zn$X$ and Co-doped Zn$X$ are displayed more clearly. For Zn$X$, the valence band is mainly contributed by the p electrons, while the conduction band consists of the hybrid s and p states. However, after Co atoms are doped into the lattice, the Co 3d states play an important role in the valence band around the Fermi level, as marked by the stars in Fig.3. And it can be seen from Fig.3(d), in the case of ZnS:Co, the d states around the valence band are almost composed of all the Co d states. So, it can be concluded that for the Co-doped materials, the reduction of lattice constants results in the whole energy levels (include the Fermi level) shifting down, but this does not change the band gap directly. At the same time, the energy level of Co 3d electrons is located in the band gap, leading to the modification of the Fermi level itself and thus the width of the band gap.

## 3.3. Optical properties

We will show the frequency-dependent optical properties of the zincblendes ZnX (X=S, Se, Te) and how Co doping influences the optical properties. In general, many physical parameters can be used to describe optical properties, including the complex refractive index, absorption coefficient, reflectivity coefficient, optical conductivity, complex dielectric constant and so on. But these physical parameters are connected with one another, we just select the absorption coefficient and the dielectric constant in this study for the analysis.

Shown in Figs.4(a)–4(f) are the dielectric indices

of Zn$X$ and Zn$X$:Co. The large differences between the Co-doped and the undoped materials lie in the lower photon energy region (below 2eV). As can be seen from Figs.4(a),4(c),and 4(e) for ZnS, ZnSe and ZnTe, respectively, the imaginary part of the dielectric index is zero while the real part tends to be constant and almost no peaks appear. These results agree with the experimental measurements.[35−37] However, for the Co-doped materials, the dielectric index in the lower energy area changes dramatically, for both the real part and the imaginary part. Sharp peaks appear in this photon energy area. As the imaginary part is closely related with the absorption spectra, these peaks also appear in the high wavelength region of the absorption coefficient curves, as shown in Fig.5.

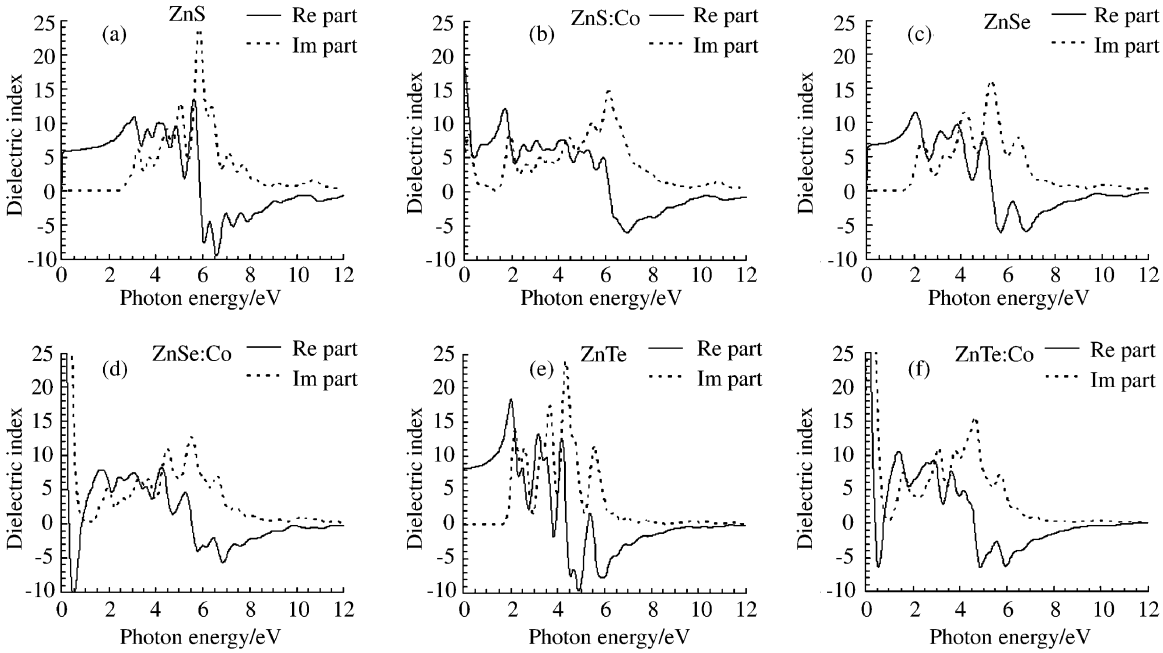
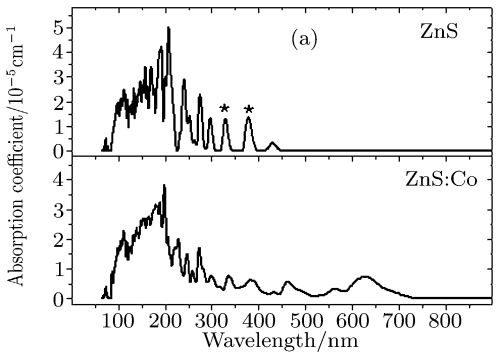
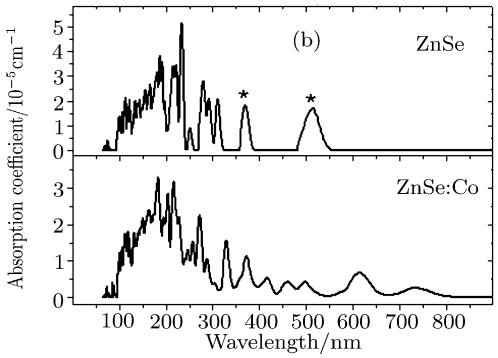



**Fig.4.** Calculated complex dielectric index of Zn$X$ and Zn$X$:Co. All of the results are calculated under [100] direction polarization.



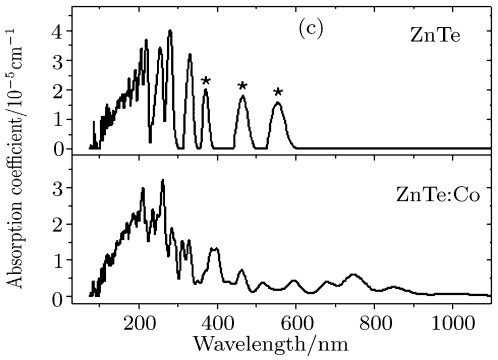




**Fig.5.** Absorption coefficient for (a) ZnS and ZnS:Co, (b) ZnSe and ZnSe:Co and (c) ZnTe and ZnTe:Co. Results are calculated under [100] direction polarization.

Shown in Figs.5(a),5(b) and 5(c) are the absorption coefficients of Zn$X$ and Zn$X$:Co calculated along [100] direction polarization. It can be seen from the figures that the shapes of the absorption curves of Zn$X$ are quite similar, except for the absorption range of ZnTe and ZnSe are extended to higher wavelengths, as compared with the ZnS case. In lower wavelength

region (below 200nm), the absorption is almost the same for the pure and Co-doped materials. This shows that the influences of the Co atom on the optical absorption of the Zn$X$ material are mainly displayed in the visible light region. At higher wavelength side (above 300nm and extended to the visible light region), the absorption peaks are very distinct and sharp, as marked by stars in the figures. However, in the case of Co-doped materials, the situation is different. The absorption peaks are no longer as sharp and distinct as the undoped materials. The peaks are lowered and the absorption ranges extend to even higher wavelengths. This shows that the band gap is decreased after Zn atoms are replaced by Co atoms in the lattice. Furthermore, the peaks in the high wavelength region upon Co doping, might be due to the d–d transition of the Co d states.

## 4. Summary

In summary, the structural, electronic and optical properties of Zn$X$ and Zn$X$:Co have been studied and compared by means of first principles calculations. Results show that the doped Co atoms reduce the lattice constant of the crystal slightly. This mainly results from the shortened Co–$X$ bond length. The local structure around the Co atom is distorted. The calculated DOS show that the band widths of the Co-doped materials are narrowed remarkably. The reason is twofold: 1) the existence of the Co 3d electron states around the Fermi level moves the valence bands up, and 2) the reduced lattice constant causes the lowering of the conduction band. In lower wavelength region, the absorption spectrum of the Co-doped Zn$X$ is almost the same as that of pure Zn$X$. However, at high wavelengths, large differences between them exist. For the case of Zn$X$, the absorption spectral peaks are sharp and distinct, while the Co-doped material has a continuum absorption spectrum which extends to even higher wavelengths.

## References


[1] Ves S, Strössner K and Gebhardt W 1986 *Phys. Rev.* B **33** 4077
[2] Dreyhsig J and Litzenburger B 1996 *Phys. Rev.* B **54** 10516
[3] Ferrer-Roca C, Segura A and Munoz V 2000 *Phys. Stat. Sol.* (a) **180** 561
[4] Zar ó nd G and Jank ó B 2002 *Phys. Rev. Lett.* **89** 047201
[5] Alvarez G, Mayr M and Dagotto E 2002 *Phys. Rev. Lett.* **89** 277202
[6] Yang S R Eric, Sinova J, Jungwirth T, Shim Y P and MacDonald A H 2003 *Phys. Rev.* B **67** 045205
[7] Maca F and Masek J 2002 *Phys. Rev.* B **65** 235209
[8] Ouyang C Y and Lei M S 2002 *Chin. J. Semicond.* **23** 1233
[9] Guo X G, Chen X S, Sun Y L, Zhou X H, Sun L Z and Lu W 2004 *Acta Phys. Sin.* **53** 3545 (in Chinese)
[10] Kuang A L, Liu X Y, Lu Z L, Ren S K, Liu C Y, Zhang F M and Du Y W 2005 *Acta Phys. Sin.* **54** 2934 (in Chinese)
[11] Rashba E I 2000 *Phys. Rev.* B **62** R16267
[12] Fert A and Jaffres H 2001 *Phys. Rev.* B **64** 184420
[13] Malajovich I, Berry J J, Samarth N and Awschalom D D 2001 *Nature* **411** 770
[14] Schmidt G and Molenkamp L W 2001 *Physica* E **10** 484
[15] Schmidt G 2005 *J. Phys.* D **38** R107
[16] Park C H and Chadi D J 2005 *Phys. Rev. Letts.* **94** 127204
[17] Li S T and Ouyang C Y 2005 *Phys. Letts.* A **336** 145
[18] Zeng Y Z and Huang M C 2005 *Acta Phys. Sin.* **54** 1749 (in Chinese)
[19] Uba S M and Baranowski J M 1978 *Phys. Rev.*B **17** 69
[20] Iwanowski R J, Jablonska K L, Golacki Z and Traverse A 1998 *Chem. Phys. Lett.* **283** 313
[21] Kresse G and Hafner J 1993 *Phys. Rev.* B **47** 558
[22] Kresse G and Furthm ü ller J 1996 *Comput. Mater. Sci.* **6** 15
[23] Payne M C, Teter M P, Allan D C, Arias T A and Joannopoulos J D 1992 *Rev. Mod. Phys.* **64** 1045
[24] Vanderbilt D 1990 *Phys. Rev.* B **41** 7892
[25] Troparevsky C, Kronik L and Chelikowsky J R 2002 *Phys. Rev.* B **65** 33311
[26] Perdew J P, Chevary J A, Vosko S H, Jackson K A, Pederson M R, Singh D J and Fiolhais C 1992 *Phys. Rev.* **46** 6671
[27] Monkhorst H J and Pack J D 1976 *Phys. Rev.* B **13** 5188
[28] Jumpertz E A 1955 *Z. electrochem.* **59** 419
[29] McMurdie H, Morris M, Evans E, Paretzkin B, Wong-Ng W, Zhang Y and Hubbard C 1986 *Powder Diffraction* **1** 345
[30] Natl. Bur. Stand (U. S.) 1964 *Monogr* **25** (3) 58
[31] Yeh C Y, Lu Z W, Froyen S and Zunger A 1992 *Phys. Rev.* B **46** 10086
[32] Tran T K, Park W, Tong W, Kyi M M, Wagner B K and Summers C J 1997 *J. Appl. Phys.* **81** 2803
[33] Tourni é E, Morhain C, Neu G, La ü gt M, Ongareto C, Faurie J P, Triboulet R and Ndap J O 1996 *J. Appl. Phys.* **80** 2983
[34] Lee S, Michl F, Rössler U, Dobrowolska M and Furdyna J K 1998 *J. Cryst. Growth* **184** 1105
[35] Ozaki S and Adachi S 1993 *Jpn. J. Appl. Phys.* **32** 5008
[36] Freeout J L 1973 *Phys. Rev.* B **7** 3810
[37] Ward L 1991 *Handbook Optical Constants Solids II* (New York: Academic Press) p737